Development 140, 1713-1719 (2013) doi:10.1242/dev.093112

UBIAD1-mediated vitamin K2 synthesis is required for vascular endothelial cell survival and development

Jeffrey M. Hegarty*, Hongbo Yang* and Neil C. Chi‡

SUMMARY

Multi-organ animals, such as vertebrates, require the development of a closed vascular system to ensure the delivery of nutrients to, and the transport of waste from, their organs. As a result, an organized vascular network that is optimal for tissue perfusion is created through not only the generation of new blood vessels but also the remodeling and maintenance of endothelial cells via apoptotic and cell survival pathways. Here, we show that UBIAD1, a vitamin K2/menaquinone-4 biosynthetic enzyme, functions cell-autonomously to regulate endothelial cell survival and maintain vascular homeostasis. From a recent vascular transgene-assisted zebrafish forward genetic screen, we have identified a *ubiad1* mutant, *reddish*/*reh*, which exhibits cardiac edema as well as cranial hemorrhages and vascular degeneration owing to defects in endothelial cell survival. These findings are further bolstered by the expression of *UBIAD1* in human umbilical vein endothelial cells and human heart tissue, as well as the rescue of the *reh* cardiac and vascular phenotypes with either zebrafish or human *UBIAD1*. Furthermore, we have discovered that vitamin K2, which is synthesized by UBIAD1, can also rescue the *reh* vascular phenotype but not the *reh* cardiac phenotype. Additionally, warfarin-treated zebrafish, which have decreased active vitamin K, display similar vascular degeneration as *reh* mutants, but exhibit normal cardiac function. Overall, these findings reveal an essential role for UBIAD1-generated vitamin K2 to maintain endothelial cell survival and overall vascular homeostasis; however, an alternative UBIAD1/vitamin K-independent pathway may regulate cardiac function.

KEY WORDS: UBIAD1, Vitamin K2, Cardiovascular development, Zebrafish, Endothelial cells

INTRODUCTION

As vertebrates undergo growth and organogenesis during their development, the vascular system must remodel in order to provide adequate blood vessels for tissue perfusion (Red-Horse et al., 2007). This vascular remodeling is achieved through a combination of endothelial cell sprouting and pruning of existing blood vessels (Domigan and Iruela-Arispe, 2012). These cellular events are regulated by angiogenic endothelial cell proliferation and migration, as well as endothelial cell apoptosis and regression, respectively (Dimmeler and Zeiher, 2000; Duval et al., 2003; Coultas et al., 2005; Carmeliet and Jain, 2011). Thus, maintaining a balance between these two processes are crucial for the maintenance of a functional vascular network, and aberrations in this dynamic endothelial cell equilibrium can lead to numerous vascular defects, including atherosclerosis, vasculitis and vascular anomalies (Tricot et al., 2000; Rajagopalan et al., 2004; Winn and Harlan, 2005). Thus, illuminating the underlying mechanisms that control vascular homeostasis may provide a greater understanding of the pathogenesis behind vascular diseases.

Previous zebrafish cardiovascular forward genetic screens have been particularly informative towards identifying genes that may regulate vascular development and homeostasis (Chen et al., 1996; Stainier et al., 1996; Childs et al., 2002; Gore et al., 2012). In particular, two recent vascular integrity mutants, *bubblehead* (Liu et al., 2007) and *redhead* (Buchner et al., 2007), which display cranial vascular hemorrhages, have provided insight as to how β-pix and Pak2a proteins may be crucial for regulating vascular integrity/maintenance through interactions with each other, as well as with other components of the endothelial cell-adhesion complex (Gore et al., 2008; Dejana et al., 2009; Zhong et al., 2011; Yoruk et al., 2012). More recent zebrafish screens have taken advantage of transgenic reporter lines to help screen for more subtle phenotypes, including specific vascular defects (Jin et al., 2007). As a result, thirty distinct vascular loci from a large-scale vascular transgene-assisted forward genetic screen were identified to affect various aspects of vascular development, including vascular integrity/maintenance. Within this group of mutants, several were noted to exhibit increased endothelial apoptosis, vascular regression and/or cranial vascular hemorrhaging. Recent positional cloning studies of one of these mutants, *tomato*, which exhibits cranial vascular hemorrhaging, revealed a crucial role for Birc2/cIap1, a member of the inhibitor of apoptosis protein family, in maintaining endothelial cell survival and blood vessel homeostasis during vascular development (Santoro et al., 2007). To investigate additional pathways that may regulate endothelial cell survival, we have further analyzed the zebrafish vascular integrity/maintenance mutant *reddish*^{s587} (*reh*), which develops a functional vasculature by 24 to 36 hours postfertilization (hpf), but then displays cranial vascular hemorrhages because of vascular degeneration by 48 hpf.

MATERIALS AND METHODS

Zebrafish strains

Embryos and adult fish were maintained under standard laboratory conditions as described previously (Chi et al., 2010). The following lines were used: *reddish*^{s587} (Jin et al., 2007), *Tg(kdrl:mcherry-ras)*^{s896} (Chi et al., 2008a), *Tg(kdrl:gfp)*^{s843} (Jin et al., 2005), *Tg(gata1:dsred)*^{sd2} (Traver et al., 2003), *Tg(fli1a:nEGFP)*^{y7} (Roman et al., 2002) and *Tg(kdrl:ubiad1)*^{sd23}.

Mapping

Positional cloning of *reddish* mutant and UBIAD1 sequence alignment by ClustalW multi-sequence alignment were performed as described previously (Chi et al., 2010).

Department of Medicine, Division of Cardiology, University of California, San Diego, La Jolla, CA 92093-0613J, USA.

*These authors contributed equally to this work
‡Author for correspondence (nchi@ucsd.edu)

Accepted 21 January 2013

Morpholino knockdown and *UBIAD1* rescue studies

To knock down *ubiad1* function, we used an antisense morpholino oligonucleotide targeted against the 5′ splice site of exon 2: 5′-GAAGCCAATCGGTATATTCACCTCC-3′. Five base pairs (bp) of this splice morpholino was altered to create a control 5 bp mismatched morpholino, which did not cause any discernible phenotypes. One-cell stage embryos were injected with 8-10 ng of *ubiad1* MO (*n*=203) or control MO (*n*=174). For mRNA rescue experiments, one cell stage *reh*$^{-/-}$ and wild-type (control) sibling embryos were injected with 100-150 pg of wild-type zebrafish *ubiad1* mRNA (*n*=87, *reh*$^{-/-}$, 83 wild type), *red*^{s587} *ubiad1* mRNA (*n*=31, *reh*$^{-/-}$, 45 wild type) or human *UBIAD1* mRNA (*n*=50, *reh*$^{-/-}$, 52 wild type) as described previously (Chi et al., 2010). For zebrafish myocardial-specific *ubiad1* rescue studies, *cmlc2:ubiad1* was generated by cloning *ubiad1* downstream of the *cmlc2* promoter in the pISceI vector as previously described (Chi et al., 2008a) and was then injected into *reh* mutants, which resulted in *ubiad1* expression throughout the myocardium (*n*=30). Because *ubiad1* was not expressed throughout all endothelial and endocardial cells by injecting with *kdrl:ubiad1*, which was generated by cloning *ubiad1* downstream of the *kdrl* promoter in the pISceI vector, zebrafish endothelial/endocardial-specific *ubiad1* rescue experiments were performed by generating a stable *kdrl:ubiad1* transgenic line, *Tg(kdrl:ubiad1)*^{sd23}, and crossing it into the *reh* mutant background (*n*=37) as previously described (Chi et al., 2008a). Bright-field and fluorescence microscopy were used to determine whether the experimental embryos exhibited the *reh* mutant cardiovascular defects. Treated embryos that exhibited no vascular/hemorrhage and cardiac defects up to 1 week later were scored as rescued. If they displayed any of these phenotypes by 48 hpf when the *reh* phenotype occurs, they were scored as unsuccessfully rescued. Rescue calculations were performed based on rescuing only genotyped *reh*$^{-/-}$.

Expression analysis and RT-PCR

Whole-mount *in situ* hybridization was performed on 24, 36, 48 and 72 hpf zebrafish embryos as described previously (Chi et al., 2008b), using a *ubiad1* RNA probe. The *ubiad1* RNA probe was generated by PCR, using the primers zF 5′-atgcaggagatgaagccggctgc-3′ and zR 5′-gtaatacgactc-actatagggctcacaataacggcag-3′. *ubiad1* RT-PCR experiments were performed from RNA obtained from one-cell stage zebrafish embryos and from human umbilical vein endothelial cells and human heart tissue. Primer sequences used for zebrafish and human RT-PCR are as follows: z-ubiad1F, 5′-cttcctgtccagcctcaaac-3′; z-ubiad1R, 5′atgaggatcaccacgtctcc-3′; h-ubiad1F, 5′-tctactacctgtcccctctgaaac-3′; h-ubiad1R, 5′-ggccaaaagtga-tgaggatg-3′. These zebrafish primers were also used for RT-PCR to confirm the *ubiad1* splicing morpholino.

Microscopy and imaging

Confocal, fluorescence and bright-field microscopy, as well as live imaging of zebrafish were performed using a Nikon C2 confocal and a Leica M205 FA stereomicroscope as described previously (Chi et al., 2008a). The *Tg(fli1a:nEGFP)*^{y7} transgenic line was used to track and count endothelial cells, as well as to time-lapse image disintegrating endothelial nuclei (*n*=5 wild-type control MO, *n*=5 *ubiad1* splice MO). The *Tg(kdrl:mcherry-ras)*^{s896} and *Tg(kdrl:gfp)*^{s843} transgenic lines were used to mark and count cranial vessels in confocal projections (*n*=10 wild type, *n*=10 *reh* mutants, *n*=5 wild-type control MO, *n*=5 *ubiad1* splice MO). The *Tg(kdrl:gfp)*^{s843} transgenic line was used for confocal time-lapse imaging of trunk and tail vasculature. (*n*=10 wild-type siblings, *n*=*reh* mutant siblings).

Cell death analysis

Using an *in situ* cell death detection kit from Roche (# 2156792), *Tg(kdrl:gfp)*^{s843} vessels were examined for cell death by TUNEL staining. Specifically, zebrafish at the indicated stages were cryosectioned and then incubated in TUNEL staining solution at 37°C for 2 hours (*n*=15 wild type, *n*=15 *reh* mutants, *n*=15 coumadin treated).

Warfarin treatment

Warfarin (Sigma, # 45706) was dissolved in DMSO (Sigma, # 472301) and diluted to 1 mM with egg water (Chi et al., 2008a). Embryos were placed in a solution with 1 ml of warfarin solution and 19 ml of egg water (50 μM warfarin).

Phylloquinone, menaquinone 4 and ubiquinone rescue

Phylloquinone/PK (Sigma cat. # 47773), menaquinone-4/MK-4 (Sigma cat. # 47774) and ubiquinone (Coq10, Tishcon Corp Liquid Q LiQsorb Drops) were dissolved in DMSO/egg water solution and injected intravenously into the sinus venosus as described previously (Zhong et al., 2006). Based on a dose response and toxicity curve, 10 mM of PK, MK-4 or ubiquinone was used to inject into 32 hpf *reh*$^{-/-}$, wild-type and warfarin-treated wild-type (WT) zebrafish for rescue experiments. The number of zebrafish treated for each condition is as follows: WT + DMSO, *n*=100; WT + MK-4, *n*=65; WT + PK, *n*=55; WT + warfarin + DMSO, *n*=100; WT + warfarin + MK-4, *n*=81, WT + warfarin + PK, *n*=56; *reh*$^{-/-}$ + DMSO, *n*=62; *reh*$^{-/-}$ + MK-4, *n*=54; *reh*$^{-/-}$ + PK, *n*=48; and *reh* + ubiquinone, *n*=106. Bright-field and fluorescence microscopy were used to determine whether the experimental embryos exhibited the *reh* mutant cardiovascular defects.

RESULTS

reh mutants appeared indistinguishable from their wild-type (WT) siblings up to 36-48 hpf; however, by 48 hpf, the *reh* mutants displayed cranial vascular hemorrhages in multiple areas of the head (Fig. 1A-C). By 72 hpf, their cranial vascular hemorrhages appeared to consolidate in the hindbrain and they also developed cardiac edema owing to decreased myocardial function (Fig. 1D-F) (compare supplementary material Movie 1 with Movie 2). To further assess whether additional vascular hemorrhages were present in the *reh* mutant, we analyzed *reh* mutants in the *Tg(kdrl:gfp);Tg(gata1:dsRed)* transgenic background, which marks endothelial cells in green and blood cells in red, respectively. Though no significant vascular or bleeding differences between wild-type siblings and *reh* mutants were observed at 36 hpf (Fig. 1G,H), *reh* mutant cranial vessels were disrupted, leading to brain hemorrhages by 48 hpf (Fig. 1J,L,N, arrows). Furthermore, many of the *reh* intersegmental vessels started degenerating at 48 hpf (supplementary material Fig. S1) (compare supplementary material Movie 3 with Movie 4) and were frequently missing or atretic by 72 hpf (Fig. 1N,P, arrowheads); however, no hemorrhages were observed in the tail or trunk (Fig. 1H,J,L,N). As a result, these cardiovascular defects led to embryonic lethality by 120 hpf.

Despite its similar phenotype to *bubblehead* (Liu et al., 2007), *redhead* (Buchner et al., 2007) and *tomato* (Santoro et al., 2007), the *reh* mutant genetically complemented these mutants, leading us to perform positional cloning studies to further understand the molecular nature of the *reh* mutant. Through extensive genetic mapping of the *reh*^{s587} mutant (Fig. 2A), we identified a missense mutation in the *ubiad1* gene that results in a Leu65Gln substitution in a highly conserved amino acid that resides in the second predicted transmembrane region of the protein (Fredericks et al., 2011) (Fig. 2B; supplementary material Fig. S2). Though reverse transcription (RT)-PCR revealed that *ubiad1* is expressed in the zebrafish as early as the one-cell stage (supplementary material Fig. S3A), *in situ* expression analysis revealed weak *ubiad1* expression throughout the entire embryo, with stronger expression in the head by 24 hpf (supplementary material Fig. S3B), and more restricted expression in the heart (supplementary material Fig. S3C, red arrow) and head by 36-48 hpf (supplementary material Fig. S3B, arrows). Furthermore, RT-PCR in human hearts and human umbilical vein endothelial cells (HUVECs) showed that *UBIAD1* is also expressed in the human cardiovascular system, suggesting that UBIAD1 may be functionally conserved (supplementary material Fig. S3D).

To confirm that loss of UBIAD1 function can recapitulate the *reh* mutant phenotype, we knocked down *ubiad1* in *Tg(kdrl:gfp);Tg(gata1:dsRed)* zebrafish embryos using a splice morpholino (MO) (supplementary material Fig. S4). *ubiad1* splice MO-injected *Tg(kdrl:gfp);Tg(gata1:dsRed)* embryos displayed a

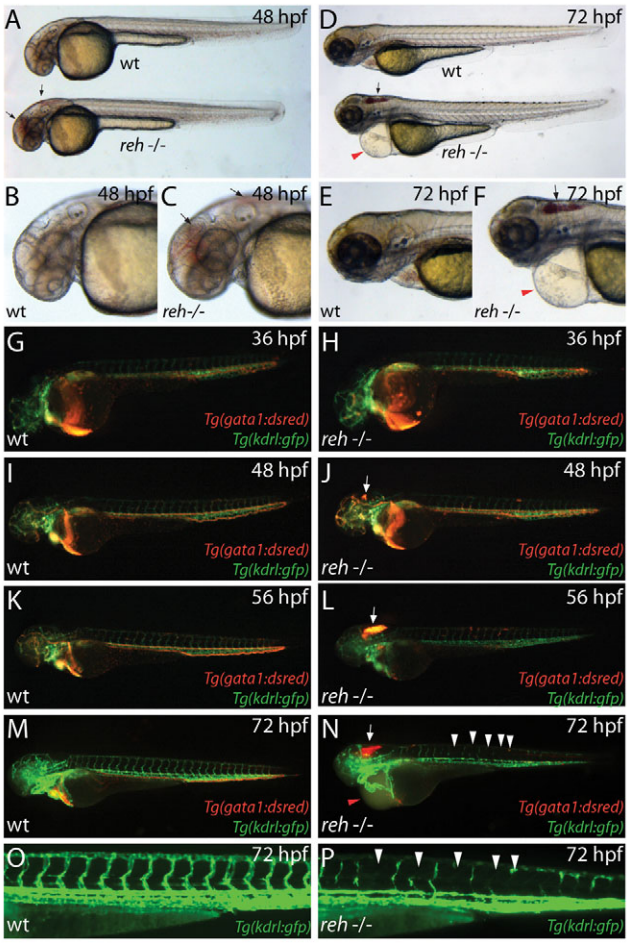

Fig. 1. *reddish*^{s587} mutants exhibit cranial hemorrhage, degenerating vessels and pericardial edema. (**A-F**) Bright-field micrographs of wild-type (wt) and *reh*^{s587} mutant (*reh*$^{-/-}$) embryos at (A-C) 48 hpf and (D-F) 72 hpf (A,C,D,F). Black arrows indicate cranial hemorrhage in *reh* mutant. Red arrowheads indicate pericardial edema. (**G-N**) Fluorescence micrographs of (G,I,K,M) wild-type (wt) and (H,J,L,N) *reh*^{s587} mutants (*reh*$^{-/-}$) in *Tg(gata1:dsRed);Tg(kdrl:GFP)* background at (G,H) 36, (I,J) 48, (K,L) 56 and (M,N) 72 hpf. Cranial hemorrhage as detected by extravasation of *Tg(gata1:dsRed)* labeled blood in the head (white arrows) occurs in *reh*^{s587} mutants as early as (J) 48 hpf and increases during development (L,N). *reh*$^{-/-}$ intersegmental vessels appear to degenerate by 72 hpf (N, white arrowheads). (**O**,**P**) *Tg(kdrl:GFP)* (O) wild-type (wt) and (P) *reh*$^{-/-}$ intersegmental vessels confirm this degeneration in *reh*$^{-/-}$ mutants at 72 hpf (white arrowheads). Red arrowhead in N indicates pericardial edema.

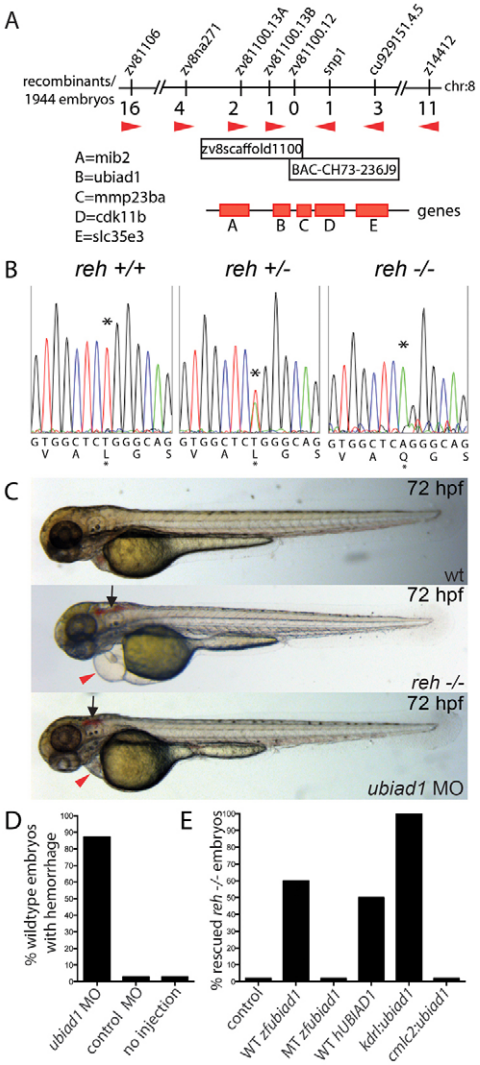

Fig. 2. *reh* encodes UBIAD1. (**A**) Genetic map of the *reh* region. Numbers below SSLP markers indicate recombination events out of 1944 diploid embryos examined. The mapped *reh* critical region contains one BAC and one genomic scaffold. (**B**) Sequencing of *ubiad1* cDNA revealed a T to A change at base pair 422 in the *s587* mutant allele, resulting in a Leu-to-Gln substitution at residue 65. Black asterisk indicates the location of the mutation. (**C**,**D**) Eighty-seven percent of wild-type (wt) embryos injected with a *ubiad1* splice morpholino exhibited cranial hemorrhage (black arrows) and mild cardiac edema (red arrowheads), but wild-type embryos injected with control morpholino displayed no discernible cardiovascular phenotypes. (**E**) Wild-type zebrafish *ubiad1* (WT *zfubiad1*) mRNA, human *UBIAD1* (WT *hUBIAD1*) mRNA and zebrafish *kdrl:ubiad1* rescued the *reh* cardiac and vascular phenotype. However, neither zebrafish *ubiad1*^{s587} (MT *zfubiad1*) mRNA nor zebrafish *cmlc2:ubiad1* could rescue either *reh* cardiovascular mutant phenotypes.

similar vascular phenotype but a milder cardiac phenotype from that of *reh* mutants (Fig. 2C,D; *n*=177/203). Conversely, injection of wild-type zebrafish and human *UBIAD1* mRNA into *reh* embryos rescued 60% (*n*=53/87) and 50% (*n*=25/50) of both *reh* cardiac and vascular phenotypes, respectively (Fig. 2E), whereas injection of zebrafish *ubiad1*^{s587} mRNA failed to rescue *reh* mutants (*n*=0/31). However, injection of these mRNAs in wild-type embryos did not cause any detectable phenotype. Vascular specific expression of zebrafish *ubiad1* (*kdrl:ubiad1*) was able to rescue 100% of both *reh* vascular and cardiac phenotypes (*n*=37/37), but, interestingly, myocardial-specific expression of zebrafish *ubiad1* (*cmlc2:ubiad1*) was unable to rescue either *reh* mutant phenotypes (*n*=0/30) (Fig. 2E). Though wild-type zebrafish and human *UBIAD1* RNA rescued *reh* mutants did not survive beyond 168 hpf owing to recurring cardiovascular defects at 120 hpf, all *kdrl:ubiad1* rescued *reh* mutants survived into adulthood, suggesting that UBIAD1 may be required throughout development. Overall, the strong genetic linkage, identification of a molecular lesion in a highly conserved amino acid residue, expression analysis, MO phenocopy and *UBIAD1* rescue studies indicate that *ubiad1* is the gene affected by the *reh* mutation.

To further understand the function of UBIAD1 during vascular development, we examined more closely the cranial vasculature of

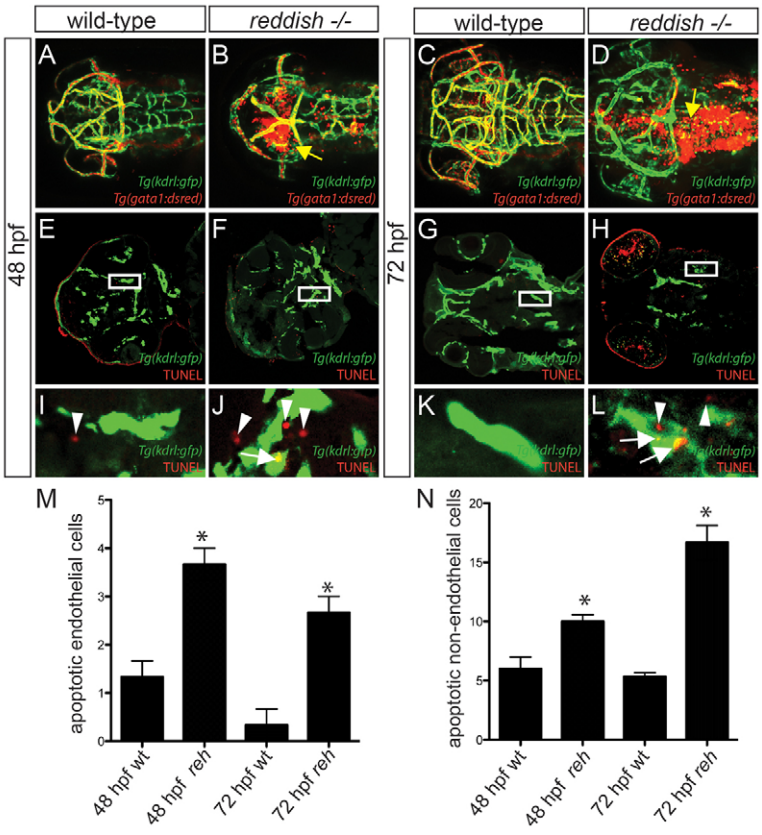

Fig. 3. Vascular integrity and endothelial survival are compromised in *reh* mutants due to increased apoptosis. (**A-D**) Confocal projections of 48 and 72 hpf *Tg(kdrl:gfp);Tg(gata1:dsRed)* (A,C) wild-type or (B,D) *reh* mutant zebrafish. Yellow arrow indicates extravasation of *Tg(gata1:dsRed)*-labeled blood. (**E-L**) Confocal sections of 48 and 72 hpf *Tg(kdrl:gfp)* wild-type (wt) and *reh* mutant zebrafish that were TUNEL stained (red) reveal that (F,H,J,L) *reh* endothelial cells exhibit increased apoptosis when compared with (E,G,I,K) wild-type endothelial cells. (I-L) Enlargements of boxed areas in E-H, respectively, show (J) increased cell death in not only *reh* endothelial cells (white arrows) but also in (L) cells surrounding these *reh* endothelial cells (white arrowheads) when compared with wild-type vasculature. (**M**,**N**) The number of apoptotic cells observed per high-power field for each condition. Mean+s.e.m. Student's *t*-test, **P*<0.05 (*n*=15 *reh* and wild-type zebrafish).

reh mutant and *ubiad1* splice MO-injected zebrafish by confocal microscopy using *Tg(kdrl:gfp);Tg(gata1:dsRed)* and *Tg(fli1a:nEGFP);Tg(kdrl:cherry-ras)* transgenic fish, respectively. Although *reh* and wild-type cranial blood vessels developed similarly at 36-40 hpf (Fig. 1G,H; supplementary material Fig. S1) (Isogai et al., 2001), we observed that many of the *reh* cranial blood vessels started degenerating by 48 hpf (compare Fig. 3A and 3B), resulting in subsequent cranial hemorrhages (Fig. 3B, yellow arrow). By 72 hpf, *reh* mutants had significantly fewer cranial vessels than wild-type zebrafish (compare Fig. 3C and 3D; supplementary material Fig. S5A), and their remaining vessels appeared atretic and contained few blood cells (Fig. 3D). To investigate how loss of *ubiad1* function leads to reduced cranial blood vessels, we examined the number of endothelial cells, as well as fragmented endothelial nuclei in *ubiad1* splice and control MO-injected *Tg(fli1a:nEGFP);Tg(kdrl:cherry-ras)* zebrafish (Siekmann and Lawson, 2007). Again, the *ubiad1* splice MO-injected zebrafish cranial vasculature exhibited atretic cranial vessels by 48 hpf (Fig. 4B) and continued to degenerate further by 72 hpf (Fig. 4D), leading to fewer overall cranial vessels (supplementary material Fig. S5B) and significantly fewer endothelial cells (Fig. 4E). Time-lapse imaging in *ubiad1* splice MO-injected zebrafish from 48 to 72 hpf revealed that this decrease in endothelial cells is probably due to increased endothelial cell karyorrhexis and apoptosis (Fig. 4D, boxed area; Fig. 4F,H; supplementary material Movie 5). TUNEL cell death assays performed in wild-type and *reh* mutant *Tg(kdrl:gfp)* zebrafish confirmed that *ubiad1* loss of function results in increased endothelial cell apoptosis at 48 and 72 hpf (Fig. 3F,H; 3J,L, arrows; Fig. 3M); however, a small, albeit significant, increase in endothelial cell death was also observed as early as 36 hpf but not at 28 hpf (supplementary material Fig. S6). In addition to the endothelial cell death, increased apoptosis in cells surrounding the *reh* endothelial cells could be detected at 48 and 72 hpf (Fig. 3F,H,J,L arrowheads; 3N), suggesting that *ubiad1* may also regulate survival of vascular support cells.

Because previous studies have shown that UBIAD1 is required for menaquinone-4/vitamin K2 biosynthesis (MK-4) (Suvarna et al., 1998; Nakagawa et al., 2010; Vos et al., 2012), we investigated whether active MK-4 may mediate the role of UBIAD1 in vascular maintenance. To achieve this, we blocked the conversion of oxidized vitamin K derivatives to its active reduced forms in *Tg(kdrl:gfp);Tg(gata1:dsRed)* zebrafish by treating with 50 μM of warfarin (Fig. 5J). As a result, warfarin treatment at 24 hpf resulted in a similar vascular phenotype to that of the *reh* mutant and *ubiad1* splice MO-injected zebrafish (Fig. 5B; supplementary material Fig. S7B,D,E). Specifically, these 24 hpf warfarin-treated zebrafish exhibited atretic cranial vasculature and hemorrhaging owing to endothelial cell apoptosis by 48-72 hpf as observed in *reh* mutants (compare Fig. 3D with Fig. 5B; compare Fig. 3F,H with supplementary material Fig. S8B,D). Unlike the *ubiad1* loss-of-function zebrafish, these warfarin-treated zebrafish did not develop a significant cardiac edema, suggesting that the vitamin K cycle may not be essential for maintaining cardiac function (supplementary material Fig. S7B,D). Interestingly, treatment of either active phylloquinone/vitamin K1 (PK) or MK-4 at 36 hpf was sufficient to rescue 75% (*n*=42/56) and 94% (*n*=76/81) of the warfarin-induced cranial hemorrhage/vascular defects, respectively (Fig. 5C,D,I), raising the possibility that active PK may be converted to active MK-4 via UBIAD1 to maintain vascular integrity (Fig. 5J).

To further investigate whether conversion of PK to MK-4 through UBIAD1 is required to mediate vascular homeostasis, we examined whether PK or MK-4 might rescue the *reh* vascular phenotype. Injection of MK-4 into *reh* mutants at 36 hpf rescued

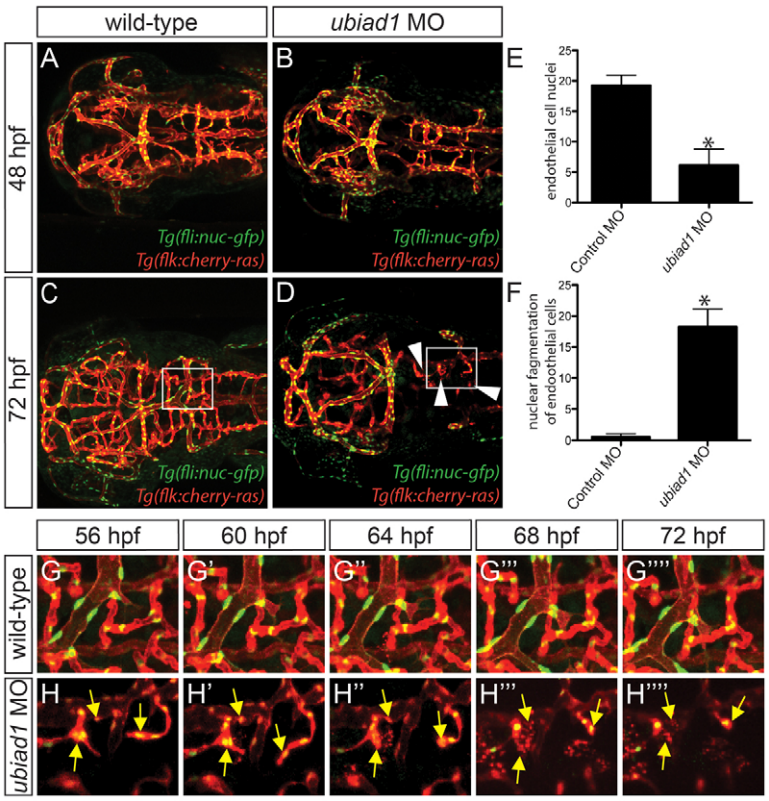

Fig. 4. Loss of *ubiad1* function results in decreased cranial vasculature and endothelial cells due to increased endothelial karyorrhexis. (**A-D**) Confocal projections of 48 and 72 hpf *Tg(fli1a:nEGFP);Tg(kdrl:cherry-ras)* (A,C) control morpholino (MO) and (B,D) *ubiad1* MO-injected zebrafish reveal that there are not only fewer *reh* endothelial cells but there is also an increase in nuclear fragmentation (karyorrhexis) in *ubiad1* morpholino-injected zebrafish when compared with control-injected animals. Arrowheads indicate missing cranial vessels. (**E**) The number of endothelial nuclei is reduced in *ubiad1* morpholino-injected zebrafish when compared with control morpholino-injected zebrafish. The number of endothelial nuclei observed per high-power field at 72 hpf. (**F**) An increase in the number of endothelial cells undergoing nuclear fragmentation was observed in *ubiad1* morpholino-injected zebrafish when compared with control morpholino-injected zebrafish. The number of endothelial nuclei undergoing karyorrhexis per high-power field from 48 to 72 hpf. Mean+s.e.m. Student's *t*-test, **P*<0.05 (*n*=5). (**G-H''''**) Time-lapse imaging of boxed areas in C (G-G'''') and D (H-H'''') shows that endothelial nuclei from (H-H'''') *ubiad1* morpholino-injected but not (G-G'''') control morpholino-injected zebrafish exhibit increased nuclear fragmentation, resulting in subsequent endothelial cell death. Yellow arrows indicate endothelial nuclei undergoing fragmentation.

58% of the *reh* vascular phenotype by 48 hpf (*n*=31/54, Fig. 5H,I), whereas injection of PK rescued only 6% (*n*=3/48, Fig. 5F,I). Specifically, MK-4 treated *reh* mutants exhibited patent and intact cranial blood vessels with no extravasation of blood at 72 hpf (Fig. 5H), whereas PK-treated *reh* mutants displayed atretic and/or absent cranial vasculature with hemorrhaging (Fig. 5F). Interestingly, some of the MK-4-rescued *reh* mutants began to display vascular degeneration and cranial hemorrhages by 72-96 hpf (*n*=15/54, 28% rescue), suggesting that sustained MK-4 production is required to maintain endothelial survival. By contrast, neither PK nor MK-4 treatment was able to rescue the *reh* cardiac phenotype, further supporting the possibility that UBIAD1 may regulate cardiac function through a vitamin K-independent pathway. Because of the similarity in the protein sequences of UBIAD1 and the *E. coli* UbiA enzyme (Bräuer et al., 2004; Orr et al., 2007; Bräuer et al., 2008; Nickerson et al., 2010), which is involved in ubiquinone biosynthesis (Boehm et al., 2000), we also tested the ability of ubiquinone to rescue the *reh* mutant phenotype but discovered that it was unable to rescue the *reh* vascular or cardiac phenotype (*n*=0/106). Overall, the combination of these warfarin and vitamin K experiments suggests that UBIAD1 preserves vascular homeostasis through a vitamin K2- but not a K1-dependent mechanism; however, UBIAD1 may regulate cardiac function through a vitamin K-independent pathway.

DISCUSSION

Although many vitamin K-dependent proteins are involved in blood coagulation (Stafford, 2005), vitamin K2/MK-4 has recently been reported to possess biological functions outside of the vitamin K canonical co-factor role (Ichikawa et al., 2006; Igarashi et al., 2007), including prevention of oxidative cell death in oligodendrocytes (Li et al., 2009) as well as an anti-apoptotic effect on erythroid lineages (Sada et al., 2010). Recent studies in *Drosophila* revealed that MK-4 may regulate mitochondrial function through its ability to transfer electrons in the electron transport chain (Vos et al., 2012). Additionally, these *Drosophila* studies also showed that UBIAD1 is required to synthesize MK-4, as recently reported (Nakagawa et al., 2010); and, moreover, MK-4, but not ubiquinone, could rescue the *Drosophila ubiad1* mutant *heixuedian* (*heix*). Using the zebrafish *reh* (*ubiad1*) mutant, we have also discovered that UBIAD1 is required to generate MK-4 for the maintenance of endothelial cell survival. Similar to the *Drosophila* data, MK-4, but not ubiquinone, is able to rescue the *reh* endothelial cell apoptosis phenotype. However, MK-4 could not rescue the cardiac dysfunction phenotype, suggesting that UBIAD1 may have additional roles beyond producing MK-4.

Recent studies have suggested that endothelial mitochondria may primarily serve roles in cellular homeostasis, such as maintaining calcium concentration (Berridge et al., 2000), generating reactive oxygen species (ROS) (Turrens, 2003) and activating signaling cascades, including apoptotic stimuli (Green and Kroemer, 2004; Green et al., 2011). In particular, siRNA-mediated knockdown of the mitochondrial mitofusin proteins, MFN1 and MFN2, in HUVECs led to not only decreased mitochondrial membrane potential and disrupted mitochondrial signaling networks but also diminished endothelial cell survival and increased apoptosis (Lugus et al., 2011), thus supporting the possibility that lack of MK-4 may perturb endothelial mitochondrial function and thereby cause endothelial cell apoptosis. Thus, it will be particularly interesting in future studies to further investigate the mitochondrial function and morphology of endothelial cells in the *reh* mutants.

The inability of MK-4 to rescue the *reh* cardiac dysfunction phenotype raises the possibility that UBIAD1 may also have an additional function beyond its role to convert PK to MK-4.

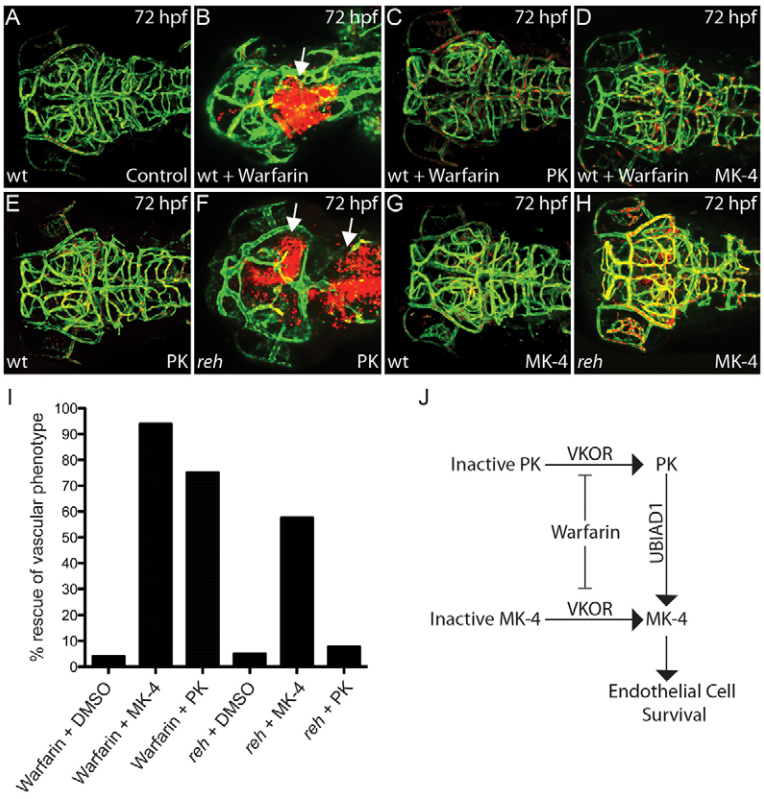

Fig. 5. UBIAD1 regulates menaquinone/vitamin K2 metabolism to maintain cranial vasculature.
(**A**,**B**) Confocal projections of (A) DMSO- and (B) warfarin-treated *reh;Tg(gata1:dsRed);Tg(kdrl:GFP)* zebrafish reveal that warfarin treatment of zebrafish at 24 hpf leads to cranial hemorrhages (white arrow) by 72 hpf. (**C**,**D**) PK (C) and MK-4 (D) treatment at 36 hpf can rescue this warfarin-induced cranial hemorrhaging and vascular defect. (**E-H**) Confocal projections of PK- and MK-4-treated *reh;Tg(gata1:dsRed);Tg(kdrl:GFP)* mutant zebrafish showed that (H) MK-4 but not (F) PK treatment at 36 hpf can rescue the *reh* vascular phenotype by 72 hpf. However, (E) PK and (G) MK-4 treatment had no discernible effect on wild-type zebrafish. Arrows in F indicate cranial hemorrhages. (**I**) MK-4 or PK treatment rescued the warfarin-induced cranial hemorrhage; however, MK-4 but not PK treatment rescued the *reh* cranial hemorrhage. (**J**) The relationship of vitamin K2/MK-4, vitamin K1/PK, UBIAD1 and warfarin.

Interestingly, *Ubiad1* is most highly expressed in mouse hearts; yet, MK-4 biosynthesis is very low or absent in this organ (Nakagawa et al., 2010). Furthermore, the localization of UBIAD1 to different subcellular domains in distinct cell types also suggests that UBIAD1 may have additional functions beyond synthesizing MK-4 (Nakagawa et al., 2010; Nickerson et al., 2010). Given that endothelial/endocardial expression of wild-type *ubiad1* was able to rescue cardiac function but MK-4 was not, these findings suggest that *ubiad1* may generate additional products, which may allow endothelial/endocardial cells to non-autonomously regulate myocardial function. One possibility may be the production of ubiquinone (Nickerson et al., 2010); however, ubiquinone treatment in *reh* mutants could not rescue the *reh* cardiac or vascular phenotypes. Thus, future UBIAD1 biochemical and enzymatic studies will be necessary to investigate whether UBIAD1 may synthesize a different steroid metabolite other than MK-4 or ubiquinone in endothelial/endocardial cells to regulate myocardial function.

The role of UBIAD1 in endothelial cell survival and cardiac function may be conserved as human *UBIAD1* is able to rescue both endothelial and cardiac *reh* mutant defects and appears to also be expressed in both human endothelial cells and hearts. Interestingly, *UBIAD1* has recently been implicated in Schnyder Corneal Dystrophy (SCD) (Orr et al., 2007; Weiss et al., 2007), and transitional cell carcinoma (TCC) of the bladder, but has not been associated with any known human cardiovascular diseases. Although no *UBIAD1* mutations have been identified in individuals with TCC (McGarvey et al., 2001), SCD is a rare autosomal-dominant disease harboring at least one of 22 different heterozygous *UBIAD1* missense mutations (Weiss et al., 2007). However, no homozygous *UBIAD1* mutations have been reported in any vertebrate animal until now, suggesting that complete loss of UBIAD1 function may lead to more severe phenotypes, such as cardiovascular defects, which may lead to fetal or neonatal demise. Thus, future human cardiovascular genetic studies examining *UBIAD1* are warranted to elucidate the role of *UBIAD1* in human cardiovascular diseases, including hemorrhagic strokes, heart failure and vascular anomalies.

Acknowledgements
We thank Neil Tedeschi and Lauren Pandolfo for expert help with the fish. We also thank Eugene Tkachenko, Jordan Shavit and Sarah Childs for generously providing the HUVECs, the *redhead* mutant and the *bubblehead* mutant, respectively.

Funding
This work was supported in part by grants from the American Heart Association to H.Y. [12POST12050080] and the National Institutes of Health to N.C.C. [HL104239 and HD070494]. Deposited in PMC for release after 12 months.

Competing interests statement
The authors declare no competing financial interests.

Supplementary material
Supplementary material available online at
http://dev.biologists.org/lookup/suppl/doi:10.1242/dev.093112/-/DC1

References
Berridge, M. J., Lipp, P. and Bootman, M. D. (2000). The versatility and universality of calcium signalling. *Nat. Rev. Mol. Cell Biol.* **1**, 11-21.
Boehm, R., Sommer, S., Severin, K., Li, S. M. and Heide, L. (2000). Active expression of the ubiA gene from E. coli in tobacco: influence of plant ER-specific signal peptides on the expression of a membrane-bound prenyltransferase in plant cells. *Transgenic Res.* **9**, 477-486.
Bräuer, L., Brandt, W. and Wessjohann, L. A. (2004). Modeling the E. coli 4-hydroxybenzoic acid oligoprenyltransferase (ubiA transferase) and characterization of potential active sites. *J. Mol. Model.* **10**, 317-327.
Bräuer, L., Brandt, W., Schulze, D., Zakharova, S. and Wessjohann, L. (2008). A structural model of the membrane-bound aromatic prenyltransferase UbiA from E. coli. *ChemBioChem* **9**, 982-992.
Buchner, D. A., Su, F., Yamaoka, J. S., Kamei, M., Shavit, J. A., Barthel, L. K., McGee, B., Amigo, J. D., Kim, S., Hanosh, A. W. et al. (2007). pak2a

mutations cause cerebral hemorrhage in redhead zebrafish. *Proc. Natl. Acad. Sci. USA* **104**, 13996-14001.
Carmeliet, P. and Jain, R. K. (2011). Molecular mechanisms and clinical applications of angiogenesis. *Nature* **473**, 298-307.
Chen, J. N., Haffter, P., Odenthal, J., Vogelsang, E., Brand, M., van Eeden, F. J., Furutani-Seiki, M., Granato, M., Hammerschmidt, M., Heisenberg, C. P. et al. (1996). Mutations affecting the cardiovascular system and other internal organs in zebrafish. *Development* **123**, 293-302.
Chi, N. C., Shaw, R. M., De Val, S., Kang, G., Jan, L. Y., Black, B. L. and Stainier, D. Y. (2008a). Foxn4 directly regulates tbx2b expression and atrioventricular canal formation. *Genes Dev.* **22**, 734-739.
Chi, N. C., Shaw, R. M., Jungblut, B., Huisken, J., Ferrer, T., Arnaout, R., Scott, I., Beis, D., Xiao, T., Baier, H. et al. (2008b). Genetic and physiologic dissection of the vertebrate cardiac conduction system. *PLoS Biol.* **6**, e109.
Chi, N. C., Bussen, M., Brand-Arzamendi, K., Ding, C., Olgin, J. E., Shaw, R. M., Martin, G. R. and Stainier, D. Y. (2010). Cardiac conduction is required to preserve cardiac chamber morphology. *Proc. Natl. Acad. Sci. USA* **107**, 14662-14667.
Childs, S., Chen, J. N., Garrity, D. M. and Fishman, M. C. (2002). Patterning of angiogenesis in the zebrafish embryo. *Development* **129**, 973-982.
Coultas, L., Chawengsaksophak, K. and Rossant, J. (2005). Endothelial cells and VEGF in vascular development. *Nature* **438**, 937-945.
Dejana, E., Tournier-Lasserve, E. and Weinstein, B. M. (2009). The control of vascular integrity by endothelial cell junctions: molecular basis and pathological implications. *Dev. Cell* **16**, 209-221.
Dimmeler, S. and Zeiher, A. M. (2000). Endothelial cell apoptosis in angiogenesis and vessel regression. *Circ. Res.* **87**, 434-439.
Domigan, C. K. and Iruela-Arispe, M. L. (2012). Recent advances in vascular development. *Curr. Opin. Hematol.* **19**, 176-183.
Duval, H., Harris, M., Li, J., Johnson, N. and Print, C. (2003). New insights into the function and regulation of endothelial cell apoptosis. *Angiogenesis* **6**, 171-183.
Fredericks, W. J., McGarvey, T., Wang, H., Lal, P., Puthiyaveettil, R., Tomaszewski, J., Sepulveda, J., Labelle, E., Weiss, J. S., Nickerson, M. L. et al. (2011). The bladder tumor suppressor protein TERE1 (UBIAD1) modulates cell cholesterol: implications for tumor progression. *DNA Cell Biol.* **30**, 851-864.
Gore, A. V., Lampugnani, M. G., Dye, L., Dejana, E. and Weinstein, B. M. (2008). Combinatorial interaction between CCM pathway genes precipitates hemorrhagic stroke. *Dis. Model. Mech.* **1**, 275-281.
Gore, A. V., Monzo, K., Cha, Y. R., Pan, W. and Weinstein, B. M. (2012). Vascular development in the zebrafish. *Cold Spring Harb. Perspect. Med.* **2**, a006684.
Green, D. R. and Kroemer, G. (2004). The pathophysiology of mitochondrial cell death. *Science* **305**, 626-629.
Green, D. R., Galluzzi, L. and Kroemer, G. (2011). Mitochondria and the autophagy-inflammation-cell death axis in organismal aging. *Science* **333**, 1109-1112.
Ichikawa, T., Horie-Inoue, K., Ikeda, K., Blumberg, B. and Inoue, S. (2006). Steroid and xenobiotic receptor SXR mediates vitamin K2-activated transcription of extracellular matrix-related genes and collagen accumulation in osteoblastic cells. *J. Biol. Chem.* **281**, 16927-16934.
Igarashi, M., Yogiashi, Y., Mihara, M., Takada, I., Kitagawa, H. and Kato, S. (2007). Vitamin K induces osteoblast differentiation through pregnane X receptor-mediated transcriptional control of the Msx2 gene. *Mol. Cell. Biol.* **27**, 7947-7954.
Isogai, S., Horiguchi, M. and Weinstein, B. M. (2001). The vascular anatomy of the developing zebrafish: an atlas of embryonic and early larval development. *Dev. Biol.* **230**, 278-301.
Jin, S. W., Beis, D., Mitchell, T., Chen, J. N. and Stainier, D. Y. (2005). Cellular and molecular analyses of vascular tube and lumen formation in zebrafish. *Development* **132**, 5199-5209.
Jin, S. W., Herzog, W., Santoro, M. M., Mitchell, T. S., Frantsve, J., Jungblut, B., Beis, D., Scott, I. C., D'Amico, L. A., Ober, E. A. et al. (2007). A transgene-assisted genetic screen identifies essential regulators of vascular development in vertebrate embryos. *Dev. Biol.* **307**, 29-42.
Li, J., Wang, H. and Rosenberg, P. A. (2009). Vitamin K prevents oxidative cell death by inhibiting activation of 12-lipoxygenase in developing oligodendrocytes. *J. Neurosci. Res.* **87**, 1997-2005.
Liu, J., Fraser, S. D., Faloon, P. W., Rollins, E. L., Vom Berg, J., Starovic-Subota, O., Laliberte, A. L., Chen, J. N., Serluca, F. C. and Childs, S. J. (2007). A betaPix Pak2a signaling pathway regulates cerebral vascular stability in zebrafish. *Proc. Natl. Acad. Sci. USA* **104**, 13990-13995.
Lugus, J. J., Ngoh, G. A., Bachschmid, M. M. and Walsh, K. (2011). Mitofusins are required for angiogenic function and modulate different signaling pathways in cultured endothelial cells. *J. Mol. Cell. Cardiol.* **51**, 885-893.
McGarvey, T. W., Nguyen, T., Tomaszewski, J. E., Monson, F. C. and Malkowicz, S. B. (2001). Isolation and characterization of the TERE1 gene, a gene down-regulated in transitional cell carcinoma of the bladder. *Oncogene* **20**, 1042-1051.
Nakagawa, K., Hirota, Y., Sawada, N., Yuge, N., Watanabe, M., Uchino, Y., Okuda, N., Shimomura, Y., Suhara, Y. and Okano, T. (2010). Identification of UBIAD1 as a novel human menaquinone-4 biosynthetic enzyme. *Nature* **468**, 117-121.
Nickerson, M. L., Kostiha, B. N., Brandt, W., Fredericks, W., Xu, K. P., Yu, F. S., Gold, B., Chodosh, J., Goldberg, M., Lu, W. et al. (2010). UBIAD1 mutation alters a mitochondrial prenyltransferase to cause Schnyder corneal dystrophy. *PLoS ONE* **5**, e10760.
Orr, A., Dubé, M. P., Marcadier, J., Jiang, H., Federico, A., George, S., Seamone, C., Andrews, D., Dubord, P., Holland, S. et al. (2007). Mutations in the UBIAD1 gene, encoding a potential prenyltransferase, are causal for Schnyder crystalline corneal dystrophy. *PLoS ONE* **2**, e685.
Rajagopalan, S., Somers, E. C., Brook, R. D., Kehrer, C., Pfenninger, D., Lewis, E., Chakrabarti, A., Richardson, B. C., Shelden, E., McCune, W. J. et al. (2004). Endothelial cell apoptosis in systemic lupus erythematosus: a common pathway for abnormal vascular function and thrombosis propensity. *Blood* **103**, 3677-3683.
Red-Horse, K., Crawford, Y., Shojaei, F. and Ferrara, N. (2007). Endothelium-microenvironment interactions in the developing embryo and in the adult. *Dev. Cell* **12**, 181-194.
Roman, B. L., Pham, V. N., Lawson, N. D., Kulik, M., Childs, S., Lekven, A. C., Garrity, D. M., Moon, R. T., Fishman, M. C., Lechleider, R. J. et al. (2002). Disruption of acvrl1 increases endothelial cell number in zebrafish cranial vessels. *Development* **129**, 3009-3019.
Sada, E., Abe, Y., Ohba, R., Tachikawa, Y., Nagasawa, E., Shiratsuchi, M. and Takayanagi, R. (2010). Vitamin K2 modulates differentiation and apoptosis of both myeloid and erythroid lineages. *Eur. J. Haematol.* **85**, 538-548.
Santoro, M. M., Samuel, T., Mitchell, T., Reed, J. C. and Stainier, D. Y. (2007). Birc2 (clap1) regulates endothelial cell integrity and blood vessel homeostasis. *Nat. Genet.* **39**, 1397-1402.
Siekmann, A. F. and Lawson, N. D. (2007). Notch signalling limits angiogenic cell behaviour in developing zebrafish arteries. *Nature* **445**, 781-784.
Stafford, D. W. (2005). The vitamin K cycle. *J. Thromb. Haemost.* **3**, 1873-1878.
Stainier, D. Y., Fouquet, B., Chen, J. N., Warren, K. S., Weinstein, B. M., Meiler, S. E., Mohideen, M. A., Neuhauss, S. C., Solnica-Krezel, L., Schier, A. F. et al. (1996). Mutations affecting the formation and function of the cardiovascular system in the zebrafish embryo. *Development* **123**, 285-292.
Suvarna, K., Stevenson, D., Meganathan, R. and Hudspeth, M. E. (1998). Menaquinone (vitamin K2) biosynthesis: localization and characterization of the menA gene from Escherichia coli. *J. Bacteriol.* **180**, 2782-2787.
Traver, D., Paw, B. H., Poss, K. D., Penberthy, W. T., Lin, S. and Zon, L. I. (2003). Transplantation and in vivo imaging of multilineage engraftment in zebrafish bloodless mutants. *Nat. Immunol.* **4**, 1238-1246.
Tricot, O., Mallat, Z., Heymes, C., Belmin, J., Lesèche, G. and Tedgui, A. (2000). Relation between endothelial cell apoptosis and blood flow direction in human atherosclerotic plaques. *Circulation* **101**, 2450-2453.
Turrens, J. F. (2003). Mitochondrial formation of reactive oxygen species. *J. Physiol.* **552**, 335-344.
Vos, M., Esposito, G., Edirisinghe, J. N., Vilain, S., Haddad, D. M., Slabbaert, J. R., Van Meensel, S., Schaap, O., De Strooper, B., Meganathan, R. et al. (2012). Vitamin K2 is a mitochondrial electron carrier that rescues pink1 deficiency. *Science* **336**, 1306-1310.
Weiss, J. S., Kruth, H. S., Kuivaniemi, H., Tromp, G., White, P. S., Winters, R. S., Lisch, W., Henn, W., Denninger, E., Krause, M. et al. (2007). Mutations in the UBIAD1 gene on chromosome short arm 1, region 36, cause Schnyder crystalline corneal dystrophy. *Invest. Ophthalmol. Vis. Sci.* **48**, 5007-5012.
Winn, R. K. and Harlan, J. M. (2005). The role of endothelial cell apoptosis in inflammatory and immune diseases. *J. Thromb. Haemost.* **3**, 1815-1824.
Yoruk, B., Gillers, B. S., Chi, N. C. and Scott, I. C. (2012). Ccm3 functions in a manner distinct from Ccm1 and Ccm2 in a zebrafish model of CCM vascular disease. *Dev. Biol.* **362**, 121-131.
Zhong, H., Wu, X., Huang, H., Fan, Q., Zhu, Z. and Lin, S. (2006). Vertebrate MAX-1 is required for vascular patterning in zebrafish. *Proc. Natl. Acad. Sci. USA* **103**, 16800-16805.
Zhong, H., Wang, D., Wang, N., Rios, Y., Huang, H., Li, S., Wu, X. and Lin, S. (2011). Combinatory action of VEGFR2 and MAP kinase pathways maintains endothelial-cell integrity. *Cell Res.* **21**, 1080-1087.

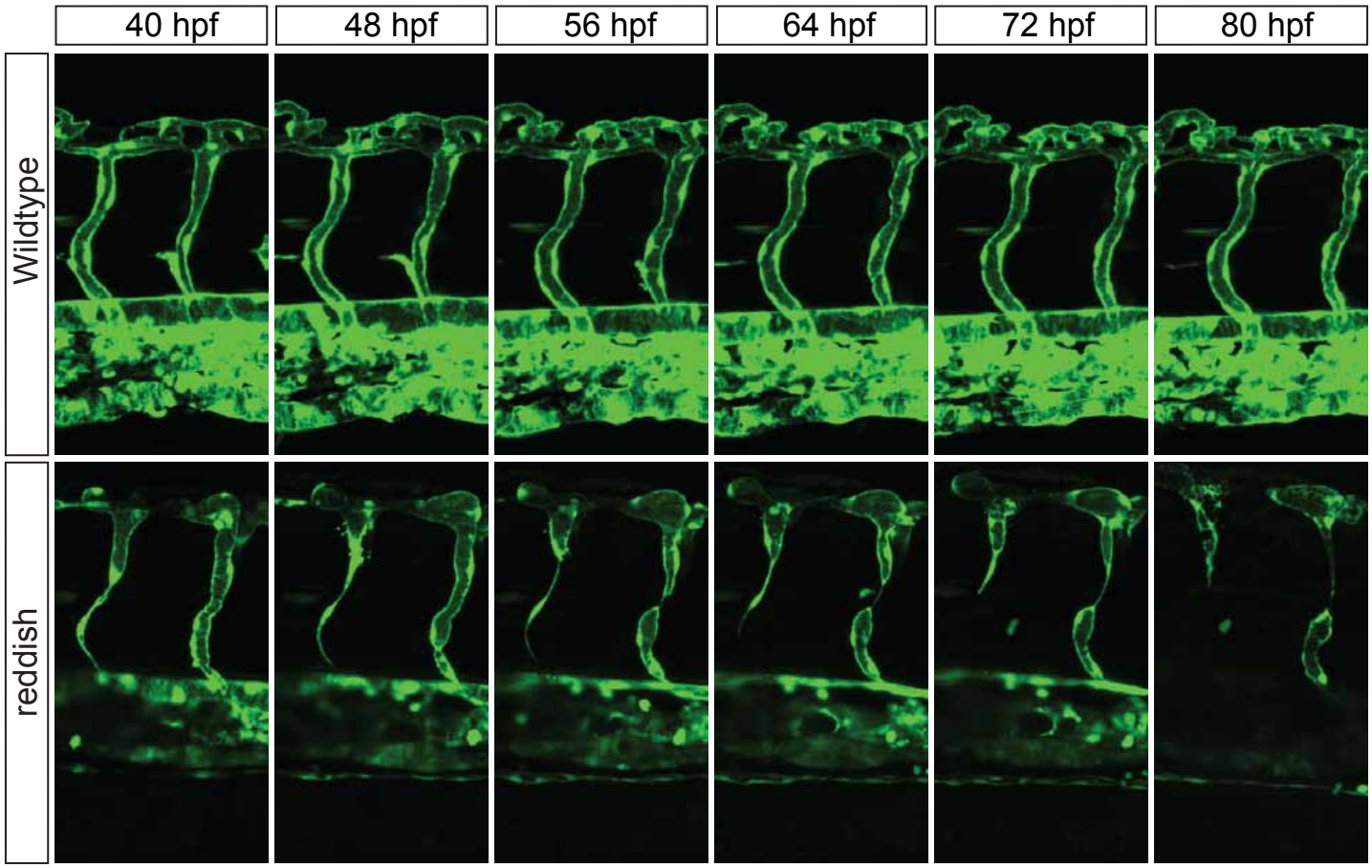

Fig. S1. The *reh* mutant intersegmental vessels start degenerating at 48 hpf and become absent or atretic by 72 hpf. Time-lapse confocal imaging of *Tg(kdrl:GFP) reh* and wild-type vasculature between 40-80 hpf shows that *reh* intersegmental vessels begin to degenerate at 48 hpf and are either absent or atretic by 72 hpf, whereas wild-type intersegmental vessels remain patent during the same time period. Time interval is every 15 minutes. Representative images are shown every 8 hours. Top, dorsal longitudinal anastomotic vessel; bottom, dorsal aorta/cardinal vein.

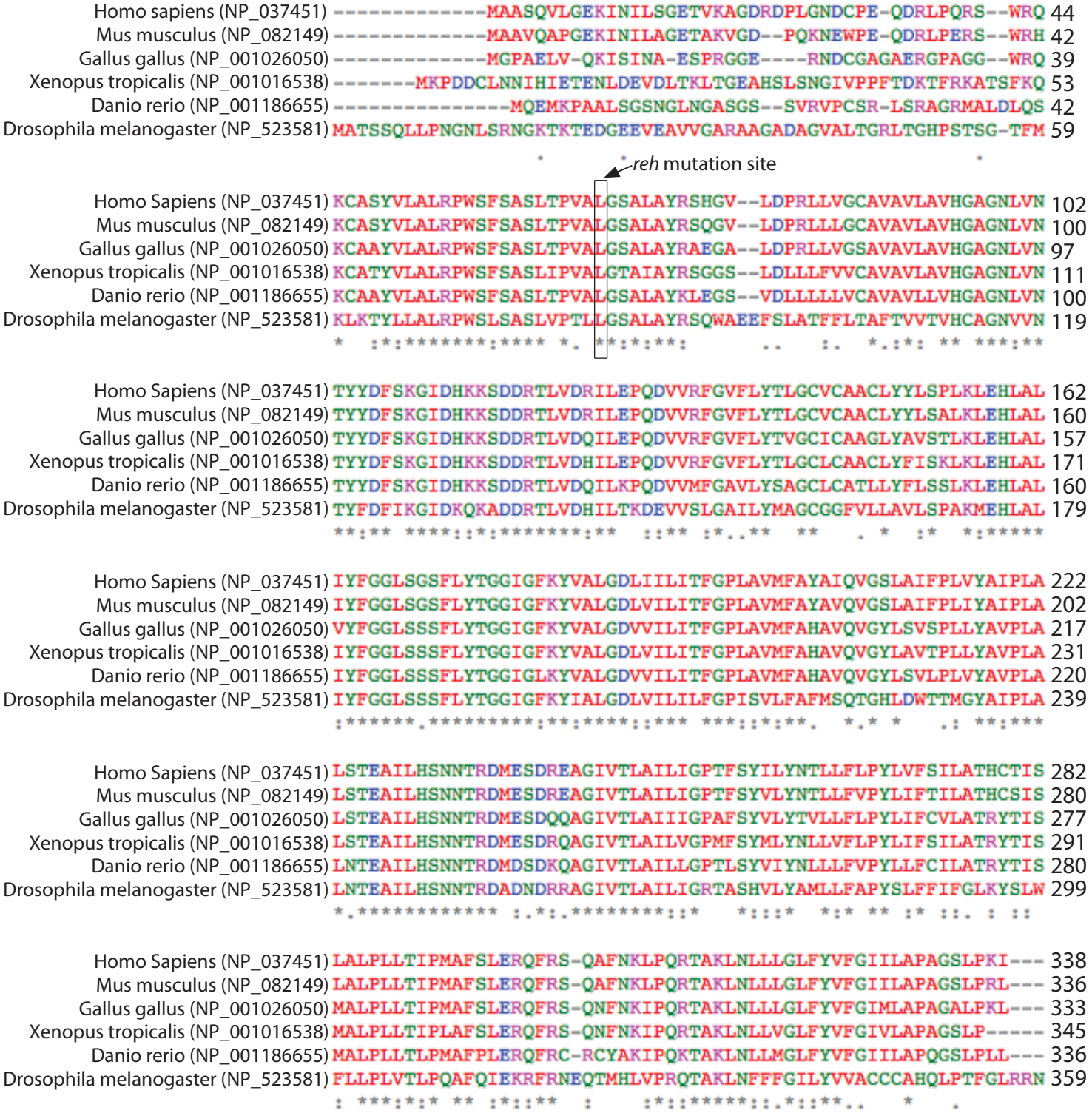

Fig. S2. Ubiad1 is conserved across vertebrate and invertebrate species. Alignment of human, mouse, chick, frog, zebrafish and fly UBIAD1 sequences. Underneath the protein sequences, identical and similar amino acids are labeled by an asterisk or a colon/ period, respectively. Zebrafish UBIAD1 and human UBIAD1 proteins share 78.9% homology. The *reh* mutation results in the amino acid change of a highly conserved amino acid (boxed amino acid) in the second transmembrane domain of UBIAD1. GenBank accession numbers used for the analysis are as follows: human UBIAD1 (NP_037451), mouse UBIAD1 (NP_082149), chick UBIAD1 (NP_001026050), frog UBIAD1 (NP_001016538), zebrafish UBIAD1 (NP_001186655) and fly UBIAD1 (NP_523581). Human, mouse, chick, frog, and fly UBIAD1 proteins are highly similar to zebrafish UBIAD1 protein.

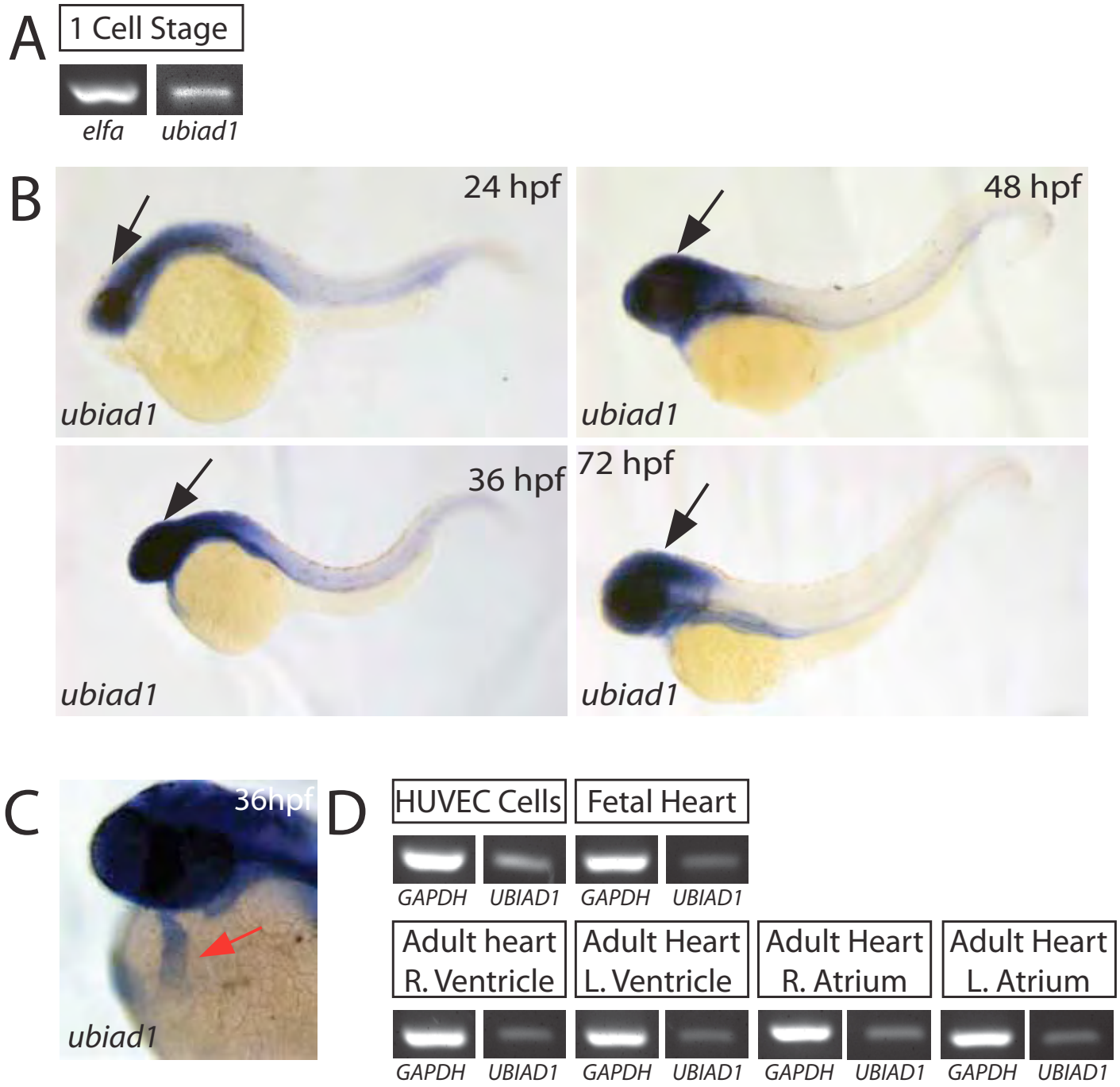

Fig. S3. UBIAD1 is expressed in the heart and vasculature. (**A**) RT-PCR shows that UBIAD1 is expressed at the one-cell stage of zebrafish embryos. (**B**,**C**) Whole-mount RNA in situ hybridization reveals UBIAD1 expression in the heart and brain. UBIAD1 is expressed in (B) the brain from 24 to 72 hpf (black arrows) and (C) the heart by 36 hpf (red arrow). (D) RT-PCR shows that UBIAD1 is expressed in human umbilical vein endothelial cells (HUVEC) and human hearts.

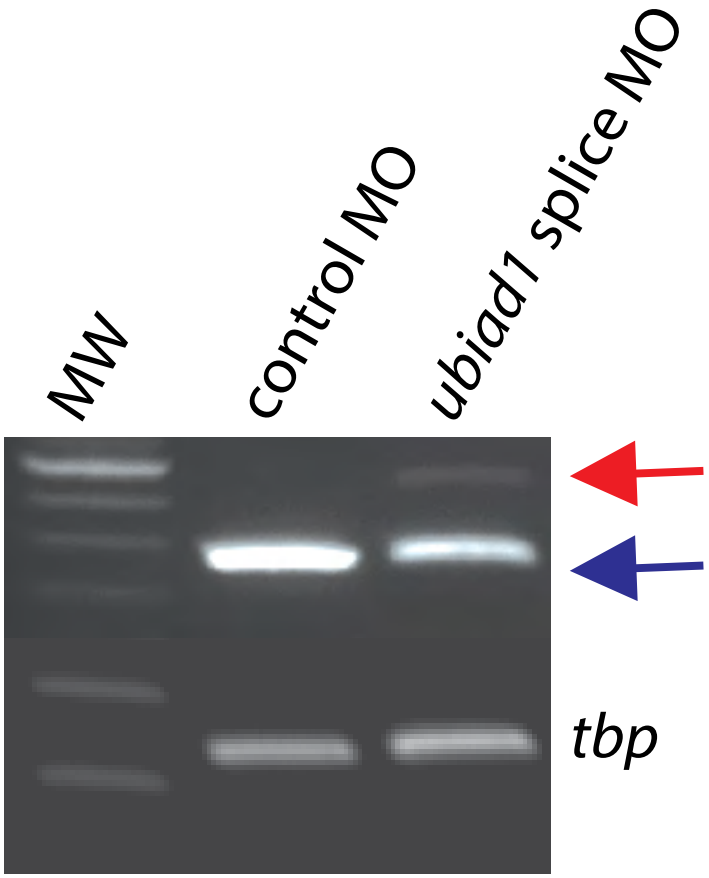

Fig. S4. Injection of *ubiad1* splice morpholino into wild-type zebrafish embryos blocks splicing of *ubiad1* RNA. Using forward 5′-ACACCTACTACGACTTCTCCA-3′ and reverse 5′-GTGATGAGGATCACCACGTCT-3′ primers to *ubiad1*, RT-PCR reveals that *ubiad1* splicing is altered in *ubiad1* splice morpholino (*ubiad1* splice MO)-injected zebrafish, but not in control morpholino (control MO)-injected zebrafish. This leads to a reduction in the levels of the correctly spliced *ubiad1* mRNA. Red arrow indicates altered splicing product; blue arrow indicates correctly spliced mRNA. *tbp* expression was used to control for *ubiad1* expression levels. MW, molecular weight marker.

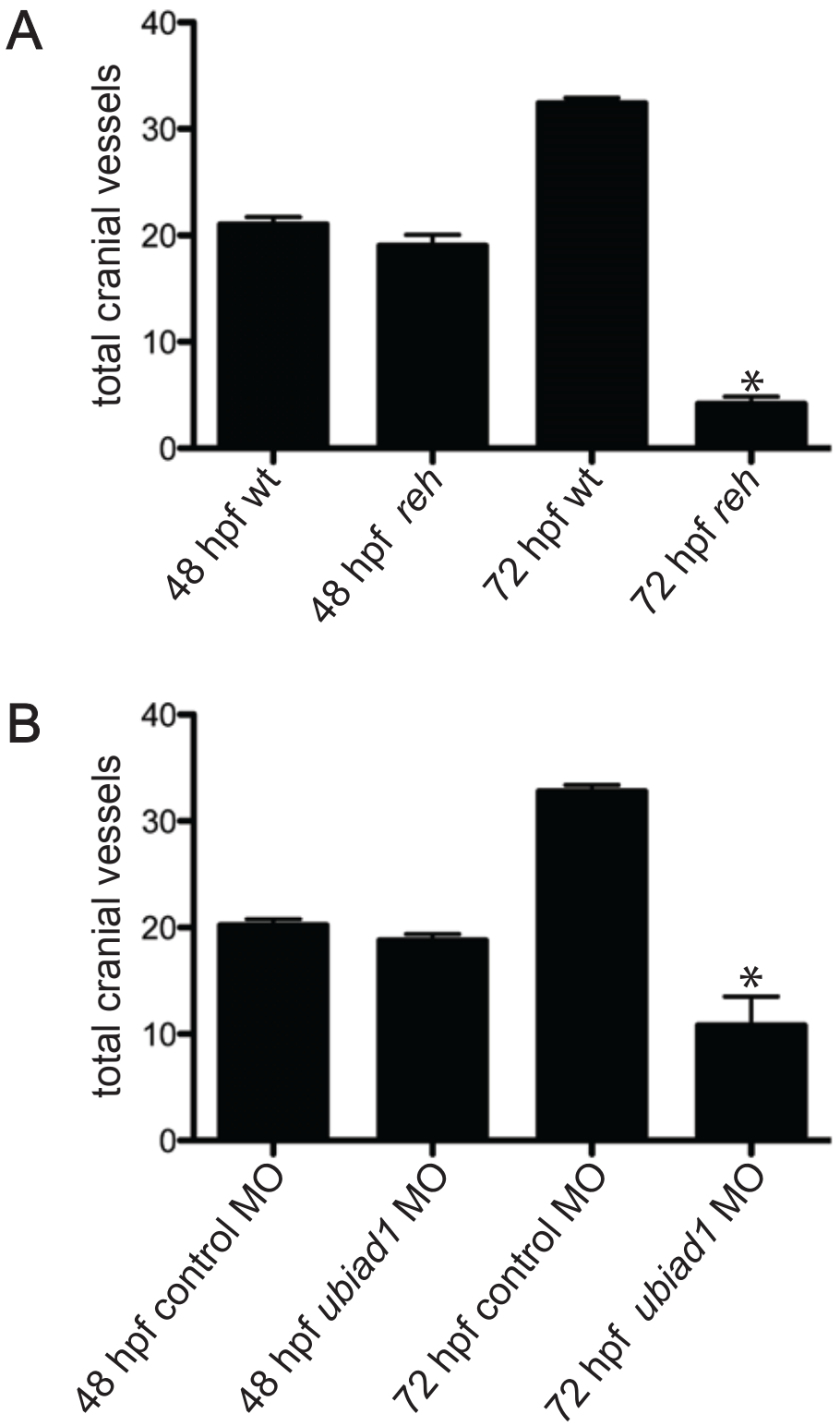

Fig. S5. *reh* mutants and *ubiad1* morpholino-injected zebrafish exhibit fewer cranial vessels than age-matched controls. Quantification of the number of cranial vessels detected on confocal projections of (**A**) *reh* and wild-type sibling control , as well as (**B**) *ubiad1* splice- and control MO-injected zebrafish at 48 and 72 hpf. Mean+s.e.m. Student's *t*-test, **P*<0.05 (*n*=10 for each condition).

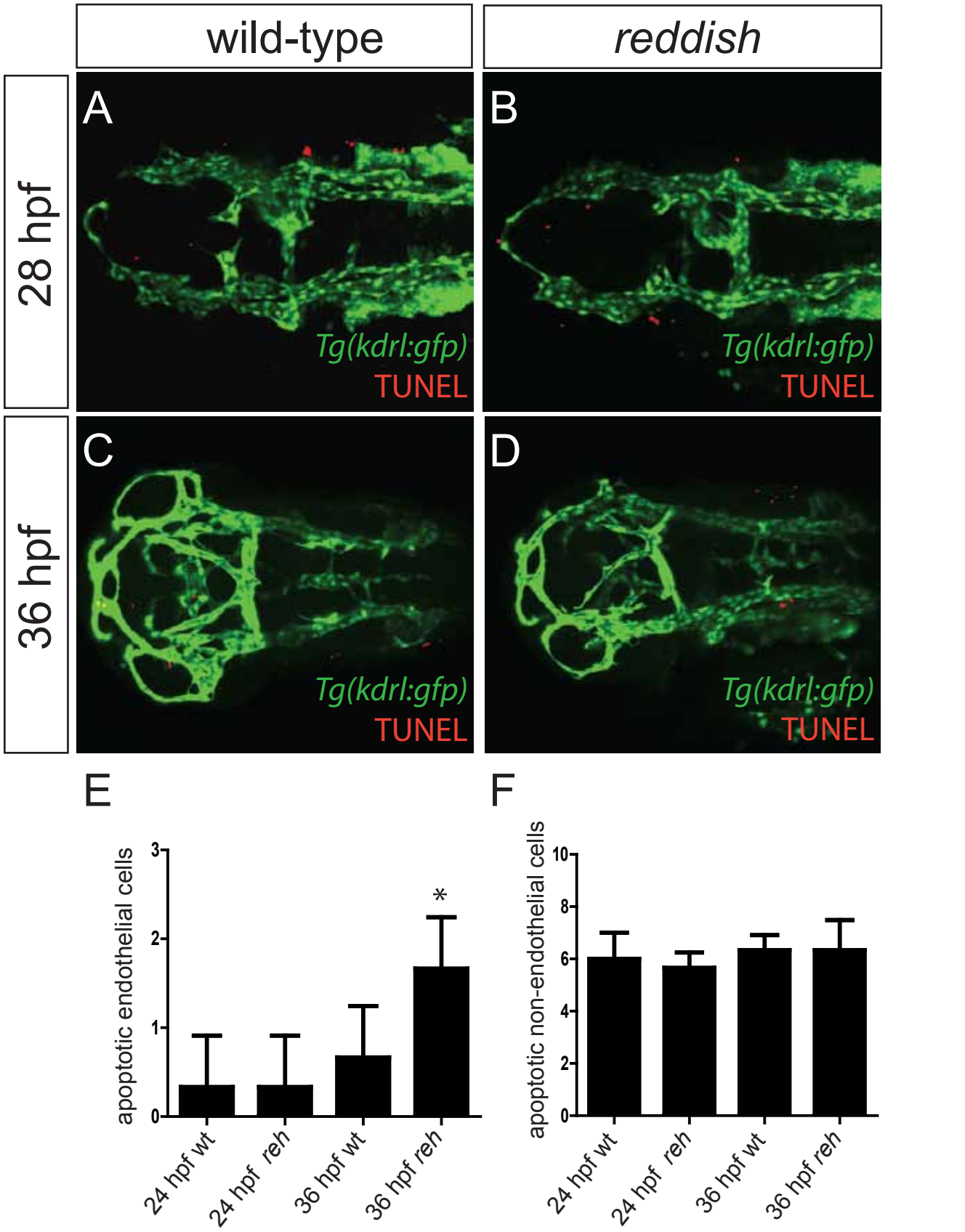

Fig. S6. Endothelial survival is compromised in *reh* mutants owing to increased apoptosis by 36 hpf. (**A-D**) Confocal projections of *Tg(kdrl:gfp)* wild-type (wt) and *reh* mutant zebrafish that were TUNEL stained (red) reveal that (D) *reh* endothelial cells exhibit increased apoptosis at 36 hpf when compared with (C) wild-type endothelial cells. However, there appeared to be no significant difference in endothelial cell death between (A) wild-type and (B) *reh* embryos at 28 hpf. (**E**,**F**) The number of apoptotic cells observed per high-power field for each condition. Mean+s.e.m. Student's *t*-test, **P*<0.1 (*n*=15 *reh* and wild-type zebrafish).

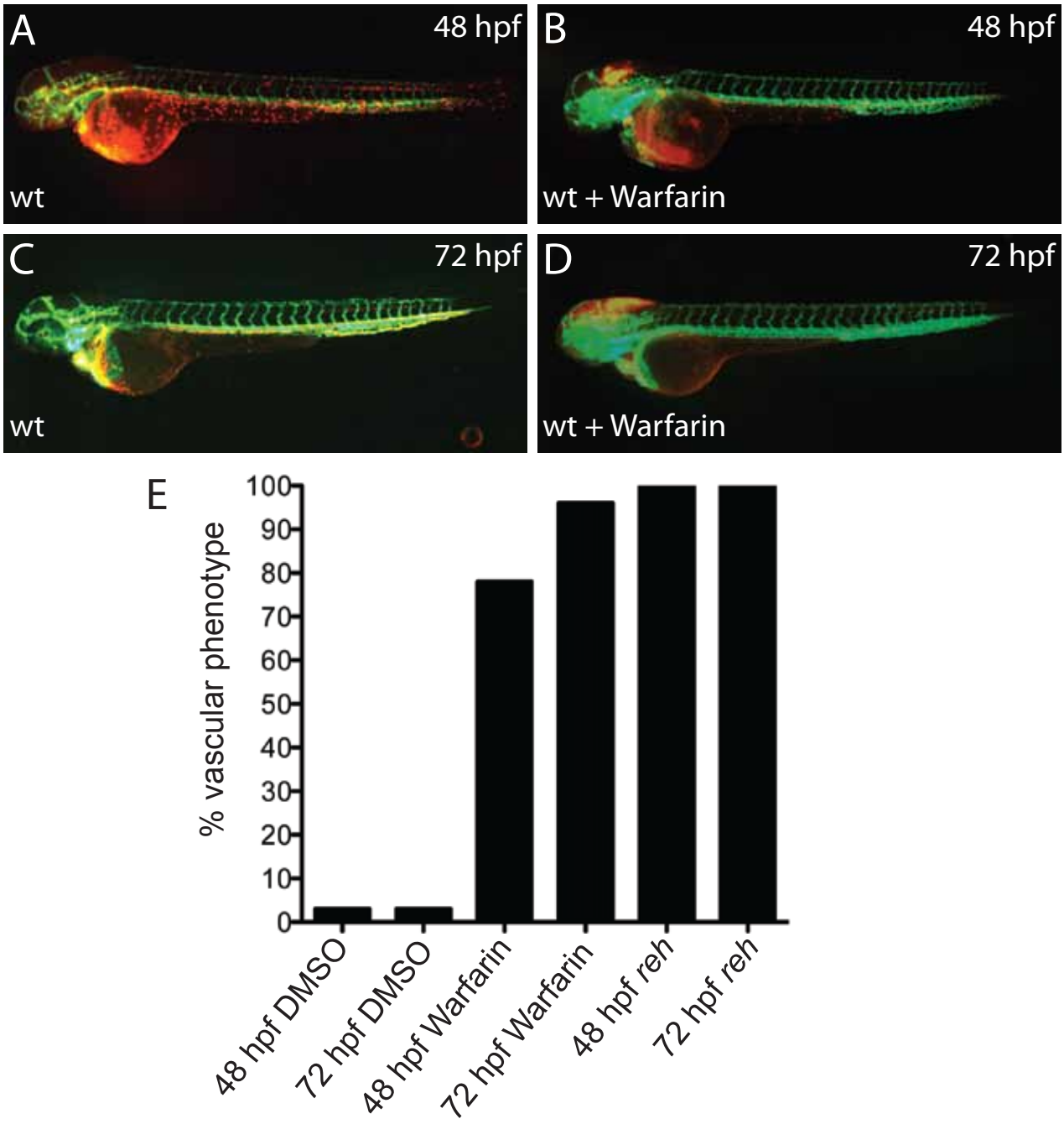

Fig. S7. Warfarin treatment of zebrafish at 24 hpf results in cranial hemorrhaging. (**A-D**) Micrographs of (A,C) DMSO- and (B,D) warfarin-treated *Tg(gata1:dsRed);Tg(kdrl:GFP)* zebrafish shows that warfarin exposure at 24 hpf can cause cranial hemorrhages by 48 and 72 hpf. (**E**) 78% of warfarin-treated zebrafish at 24 hpf displayed cranial hemorrhaged by 48 hpf, which increased to 96% by 72 hpf. All *reh* mutants but no DMSO-treated zebrafish exhibited cranial hemorrhage at 48 and 72 hpf.

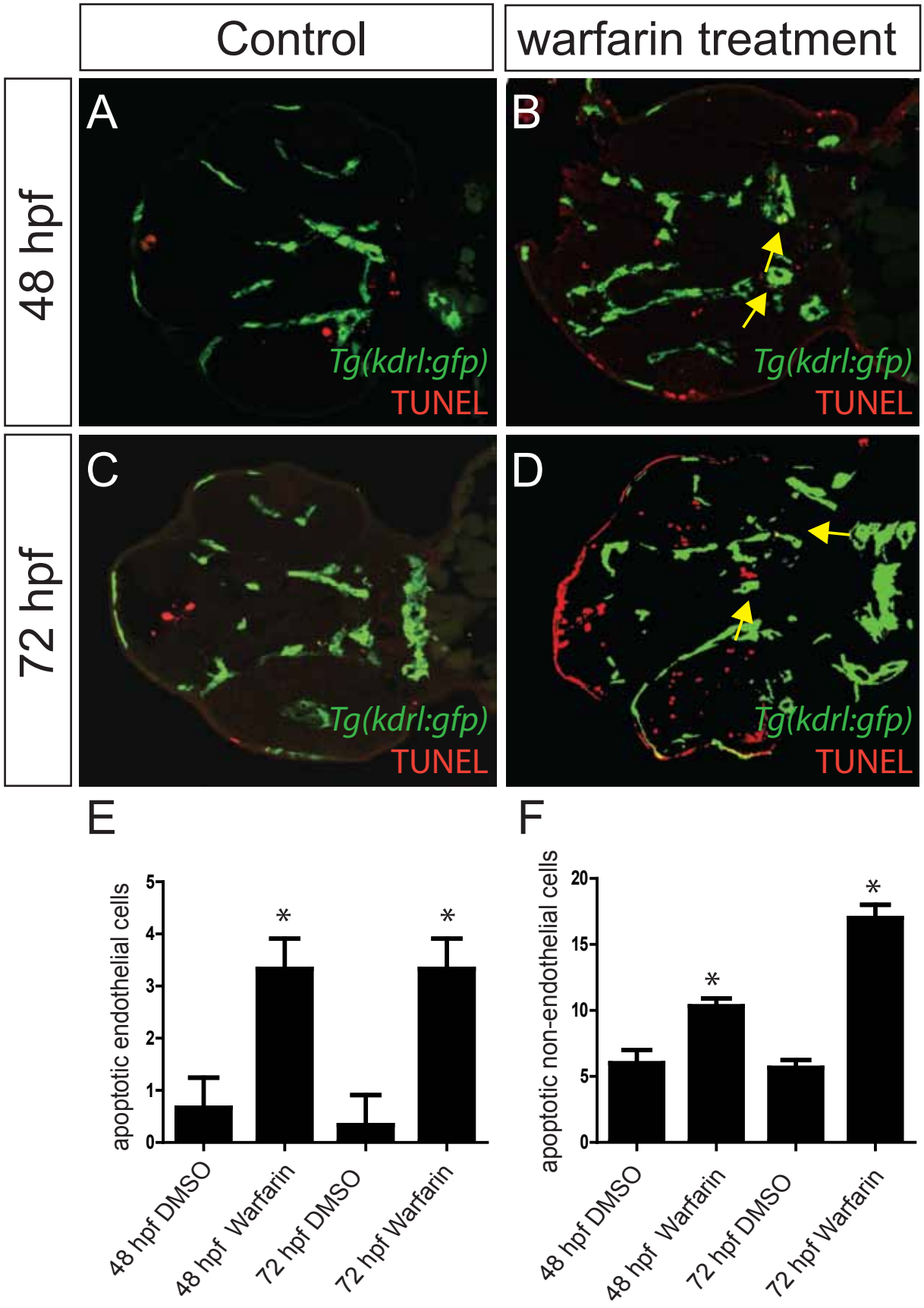

Fig. S8. Warfarin treatment of zebrafish at 24 hpf results in cranial endothelial cell apoptosis. (**A-D**) Confocal sections of 48 and 72 hpf *Tg(kdrl:gfp)* DMSO (control)- and warfarin-treated zebrafish that were TUNEL stained (red) reveal that (B,D) warfarin-treated endothelial cells exhibit increased apoptosis (yellow arrows) when compared with (A,C) control endothelial cells. (**E**,**F**) The number of apoptotic cells observed per high-power field for each condition. Mean+s.e.m. Student's *t*-test, **P*<0.05 (*n*=15 *reh* and wild-type zebrafish).

Movie 1. Cardiac function is robust in 48 hpf age-matched control. Wild-type zebrafish (48 hpf) have robust contractile function and no cardiac edema. Ventral view, anterior towards the top. Ventricle on the left and atrium on the right.

Movie 2. Cardiac function is significantly reduced in 48 hpf *reh* mutant. *reh* mutants (48 hpf) have significantly reduced contractile function leading to cardiac edema. Ventral view, anterior towards the top. Ventricle on the left and atrium on the right.

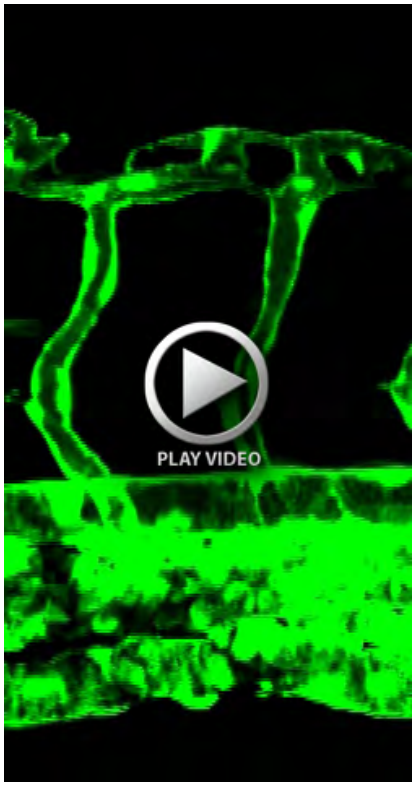

Movie 3. Time-lapse imaging of wild-type trunk vasculature reveals normal vessel development from 48-72 hpf. *Tg(kdrl:GFP)* fish were time-lapse imaged by confocal microscopy from 48-72 hpf. Time-lapse movie shows normal vascular maintenance and development. Time interval is every 15 minutes. Top, dorsal longitudinal anastomotic vessel; bottom, dorsal aorta/cardinal vein.

Movie 4. Time-lapse imaging of *reh* mutant vasculature reveals vessel degeneration from 48 to 80 hpf. *Tg(kdrl:GFP); reh* fish were time-lapse imaged by confocal microscopy from 40-80 hpf. Time-lapse movie shows degeneration of the *reh* trunk vasculature. Time interval is every 15 minutes. Top, dorsal longitudinal anastomotic vessel; bottom, dorsal aorta/cardinal vein.

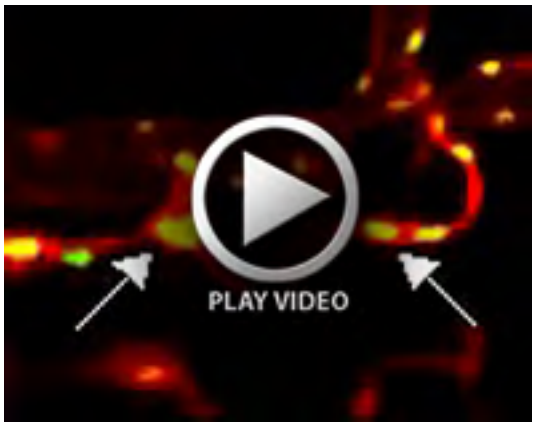

Movie 5. Time-lapse imaging of *reh* mutants reveals increased endothelial nuclear fragmentation (karyorrhexis) from 56 to 72 hpf. *Tg(fli1a:nEGFP);Tg(kdrl:cherry-ras); reh* fish were time-lapse imaged by confocal microscopy from 48 to 72 hpf. Time-lapse movie shows endothelial nuclei undergoing karyorrhexis (white arrows). Time interval is every 15 minutes.